PHYSICAL REVIEW B VOLUME 25, NUMBER 4 15 FEBRUARY 1982

Systematics of electron-hole liquid condensation from studies of silicon with varying uniaxial stress

A. Forchel, B. Laurich, J. Wagner, and W. Schmid
Physikalisches Institut, Teil 4, Universität Stuttgart, Pfaffenwaldring 57, D-7000 Stuttgart-80, Germany

T. L. Reinecke
Naval Research Laboratory, Washington, D. C. 20375
(Received 26 May 1981)

Detailed experimental results based on luminescence experiments are obtained for the ground states, the critical points, and the phase diagrams for electron-hole liquid condensation in unstressed Si and in Si with large uniaxial stresses along the [100], [110], and [111] directions, and they are shown to be in good agreement with the corresponding results from microscopic calculations also presented here. These results represent the most extensive and detailed study to date of the systematic dependences of the properties of electron-hole liquid on varying semiconductor band structure (i.e., on varying underlying energetics). The present results are used to provide the first quantitative experimental verification of scaling relations connecting the ground state and the critical properties of electron-hole liquid. Quantitative agreement is obtained with a set of scaling relations given recently by Reinecke and Ying, and systematic deviations from the predictions of earlier proposals are found. The experimental data are used to distinguish between two theoretical approaches for determining the critical point for the condensation. The values of the critical temperature are in good agreement with those obtained from a droplet fluctuation model of the condensation, but they are found to be systematically lower than those obtained from a uniform plasma model of the critical region.

I. INTRODUCTION

Following its discovery[1,2] over ten years ago electron-hole liquid (EHL) condensation has attracted a great deal of experimental and theoretical interest.[3,4] Because of the accuracy of the effective-mass approximation in semiconductors the ground-state energy and other properties of the EHL can be calculated in detail based on theoretical approaches developed for interacting electronic systems. Experimentally, a number of techniques, most particularly luminescence spectroscopy, allow an especially direct determination of the corresponding properties of the EHL. Therefore this system provides the best testing ground known for our understanding of interacting electronic systems. In addition, this unique Fermi condensation involves the most quantum fluid known.

The most complete picture of the condensation is provided by the liquid-gas phase diagram (Fig. 1) which is a curve in the density-temperature plane separating a low-density gas phase and a high-density electron-hole liquid phase from a phase in which the two coexist. Whereas earlier work on EHL focused on the low-temperature (ground-state) properties in the elemental systems Ge (Refs. 5 and 6) and Si (Refs. 6–8), more recent work has been directed towards the thermodynamic properties of EHL including the phase diagram and its critical point.[3,4] In addition, EHL has recently been observed in a variety of indirect gap semiconductor systems including strained Ge (Ref. 9) and Si (Refs. 10 and 11) and a number of compound systems. To date, however, quantitative experimental results have been limited to the cases of Ge and unstressed Si. In particular complete phase diagrams have been measured only for Ge (Refs. 12 and 13) and for Si (Refs. 14 and 15) and with somewhat lower accuracy for stressed Ge (Ref. 9).

Because of the limited scope of quantitative experimental results to date, there is as yet no detailed, systematic picture of the variations of the ground-state and thermodynamic properties of EHL for widely varying systems. Variations in the EHL properties occur for the most part because of varying band structure. From the work of Pikus and Bir[16] and of Hensel and Feher[17] it is known in

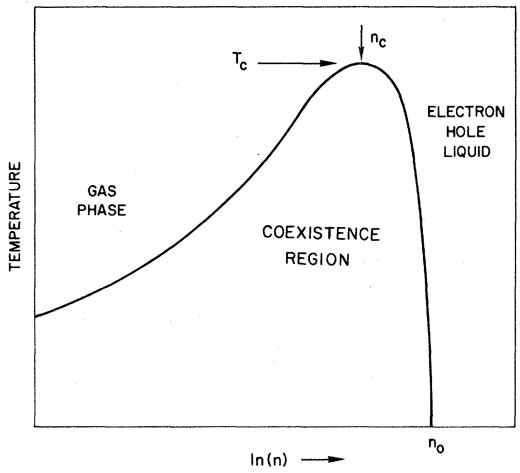

FIG. 1. Phase diagram of electron-hole liquid condensation (schematic).

detail that uniaxial stress provides an effective tool to change systematically the electronic band configuration. The application of high uniaxial stress on Si lifts progressively the conduction- and valence-band degeneracies (Fig. 2). Unstressed Si has six degenerate conduction-band minima and a twofold-degenerate valence band (denoted Si[6;2]). For large uniaxial stress along the [100], [110], and [111] directions the systems Si[2;1], Si[4;1], and Si[6;1] are obtained, respectively. In addition to the change in band degeneracy, uniaxial stress reduces the density of states of holes D_h. For the EHL the amount of the reduction depends on the ratio of the valence-band splitting ΔE_V to the hole Fermi energy E_{Fh}. In the low-stress case ($\Delta E_V/E_{Fh} < 1$) the valence-band dispersion is nonparabolic. Holes with an energy smaller than ΔE_V occupy the upshifted $|m_j| = \frac{1}{2}$ valence band, and $D_h(E)$ is significantly reduced compared to the zero-stress case. For energies larger than ΔE_V states from both valence bands are occupied and $D_h(E)$ approaches the zero-stress value.[18] In this low-stress limit the density-of-states mass of holes m_{dh} is strongly energy dependent. At high stresses ($\Delta E_V/E_{Fh} > 1$) the holes occupy only the upper valence band. The hole dispersion is parabolic and m_{dh} is independent of energy. In this "infinite-stress" limit m_{dh} is reduced by a factor of about 2 compared to the case of no stress (Table I).[17] The effects of stress on the effective total density-of-states mass of electrons m_{de} depend strongly on the stress direction (Table I). They are due to changes in the conduction-band degeneracy while the electronic density of states of each valley remains unchanged.[4]

For the investigation of the systematic variations of the EHL parameters with varying band structure we use a set of four systems given by unstressed Si and the three infinite-stress configurations. Using unstressed and highly stressed Si instead of different indirect-gap compound semiconductors has the advantage that all band structure and material parameters are known well, and corrections due to, e.g., electron-LO phonon cou-

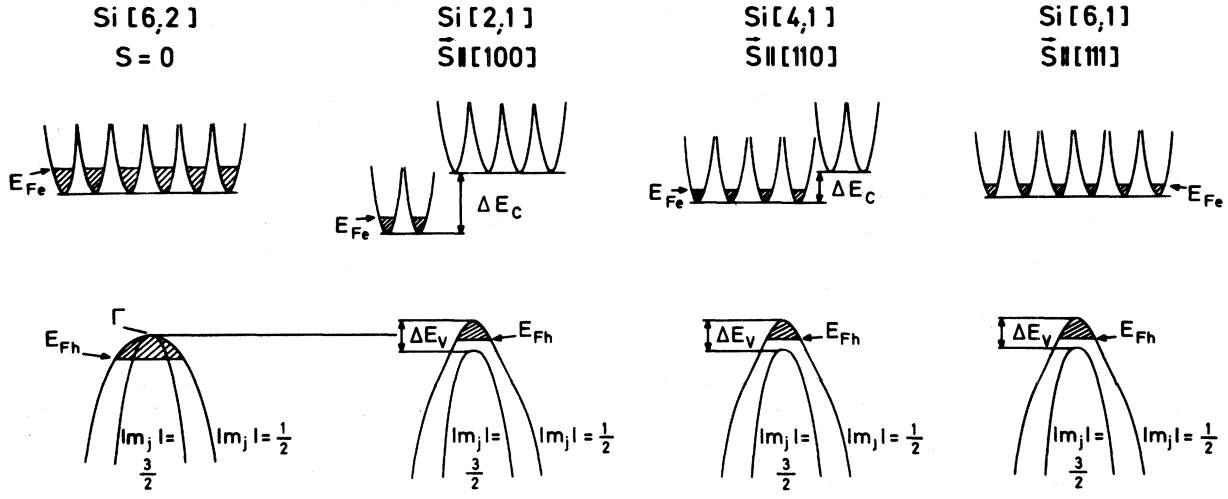

FIG. 2. Band structures of the four Si configurations obtained for unstressed Si and for Si under high uniaxial stress along its principal crystallographic axes (schematic). The Fermi energies of electrons and holes E_{Fe}, E_{Fh} in the EHL are indicated (see text).

TABLE I. Values of the total effective density-of-states masses (including band degeneracy) of electrons and holes in unstressed Si and in Si under high uniaxial stress.

	Si[6;2]	Si[6;1]	Si[4;1]	Si[2;1]
m_{de}	1.0618	1.0618	0.8103	0.5105
m_{dh}	0.577	0.2644	0.2568	0.2358

pling can be neglected.[19]

Experimentally we have developed a new method to determine directly when infinite-stress conditions are reached. This method consists of measurements of the critical temperature for electron-hole liquid condensation as a function of stress. From it we derive the amount of stress necessary to reach effectively the infinite-stress limit for the measurements of the complete phase diagrams and hence to obtain experimental data which can be compared quantitatively to theory.

Using the experimental results for the ground states, critical points, and phase diagrams obtained for widely varying band structures we are able to test quantitatively several important theoretical predictions. These include the forms of general scaling relations and different approaches for the calculation of the critical point. The present experimental results are used to give the first systematic experimental test of scaling relations between the ground-state and critical properties of EHL. The first such proposals were based on the "principle of corresponding states" for classical gases[20] and on early experiment,[3,21] and a later set was developed based on a description of the EHL at the critical point as a dense electron-hole plasma.[22] Our results provide quantitative verification of the later relations and show that there are systematic deviations from the former.

Two methods have been proposed to calculate aspects of the thermodynamic properties of EHL. The simple uniform-plasma approach allows one to calculate the critical point based on the properties of a dense interacting electron-hole system.[23,24] The droplet fluctuation approach gives the entire phase diagram as well as the critical point and includes the effects of statistical fluctuations.[25,26] Results for the critical points from both theoretical approaches are given here for these four systems and are compared to experiment. The uniform-plasma approach is found to give a consistent upper bound for the critical temperature, and the droplet-fluctuation approach gives remarkably accurate values of the critical temperature.

This paper is organized as follows. Section II gives a description of the experimental setup. Section III reports direct measurements of the stress dependence of the critical temperature, which are used to define experimentally the infinite-stress limit. In Sec. IV details of the procedure to determine the densities of the liquid phase and the gas phase are reported. Section V briefly reviews characterisitic features of the droplet-fluctuation model and the uniform-plasma model and gives theoretical results for the ground states and critical points. In Sec. VI theoretical and experimental data are compared emphasizing scaling relations and systematic changes of the EHL properties with varying stress configuration. A preliminary report of parts of the present work has already been published elsewhere.[27]

II. EXPERIMENTAL APPARATUS

For our experiments a modified He-vapor bubble cryostat has been used (Fig. 3).[28] This type of a temperature-controlled Dewar is basically a standard immersion cryostat with the He reservoir divided into two chambers. The main reservoir is situated above a polyurethane displacer which separates it from the sample chamber. Experiments at temperatures equal to (or lower than) 4.2 K can be performed in liquid or pumped He. In order to reach higher temperatures the heater of the sample chamber vaporizes the liquid He in the tail section below the displacer and heats the He vapor and the sample holder to the required temperature. Finally, this temperature is maintained by the stationary equilibrium between the flow of cold He vapor from the reservoir and the heater power.

This cryostat is particularly suitable for the present investigations because of the following.

(1) The cooling efficiency of saturated He vapor is higher than that of He gas used with standard evaporation cryostats.[28] A high cooling efficiency is of particular importance for the experimental determination of EHL phase diagrams because of the high excitation intensities required for liquid formation in the temperature region near T_c.

(2) The sample holder of the vapor-bubble cryostat can be modified easily in order to apply high and variable uniaxial stress (Fig. 3) to the samples.

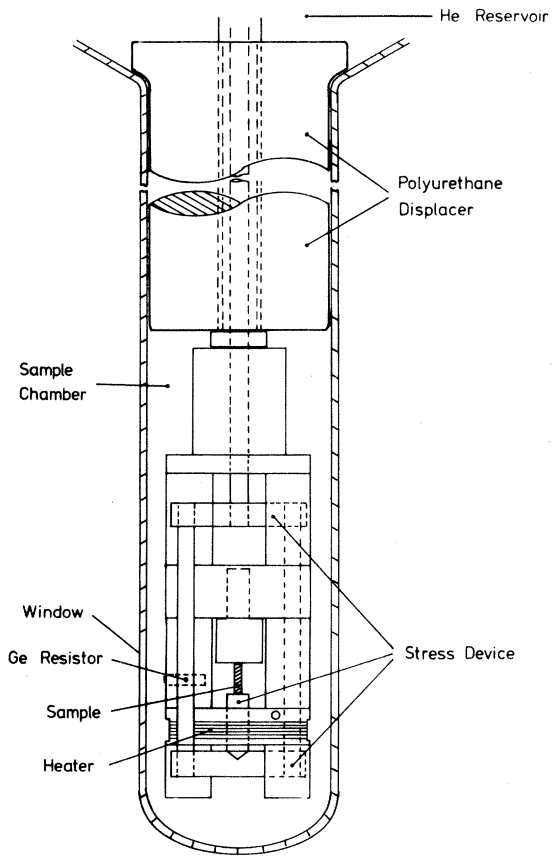

FIG. 3. Helium reservoir and sample chamber of a vapor bubble cryostat. For uniaxial stress experiments the force of a spring mounted on the top of the cryostat is transmitted by a pull rod to the stress device. For clarity the liquid-nitrogen reservoir and the vacuum tank are not shown.

Details of a stress device similar to ours have been published by Balslev.[29]

A Leybold-Heraeus high-precision temperature controller in conjunction with a calibrated Ge resistor was used to measure and stabilize the He-vapor temperature. The experiments were performed in the temperature range between 1.7 and 40 K with a typical average temperature stability of better than 0.1 K.

For our experiments 15 ns light pulses ($\lambda=514.5$ nm) at a repetition rate of 50 kHz from a cavity-dumped Ar^+-ion laser were focused on the samples in a spot of approximatively 100 μm diameter. For measurements at zero stress a sample shaped as a Weierstrass sphere ($\rho=6$ mm) was used. The stressed samples were cylindrical ($\rho=0.6$ mm, $l=10$ mm). All samples were made of high-purity n-type Si with a specific resistance of 7000 Ω cm. For the excitation of the samples peak powers of $\cong 100$ kW cm^{-2} were used. The luminescence was collected from the sample face opposite to the excitation spot and was dispersed by a 1-m Spex monochromator equipped with a grating blazed at $\lambda=1$ μm. Finally, the emission was detected by a sensitive S1 photomultiplier tube (EMI 9684B) and was processed by a fast time-resolved photon-counting system (time resolution better than 10 ns) interfaced with a computer.

Special care was taken in order to ensure high-stress homogeneity, which is essential for the present high-stress experiments ($S \leq 7$ kbar). Between the push rods of the stress device and the samples, thin pads of lead solder or indium were placed to minimize stress inhomogeneities which result from minor defects of the stressed faces of the samples. Furthermore, the cylindrical shape of the samples avoided stress gradients due to crystal edges. The stress homogeneity was monitored by time-resolved analysis of the free-exciton (FE) luminescence. Significant stress gradients within dimensions comparable to the exciton diffusion length lead to a migration of the excitons towards the region of maximum stress.[30] This causes the FE emission to shift to lower energies as a function of time. For the evaluation of the present data only experiments with negligible (≤ 0.2 meV in typically 200 ns) shift of the FE were considered. A further test of the stress homogeneity is given by the TO-LO phonon replicas of the FE luminescence. At low temperatures and for weak excitation intensities the TO and LO replicas of the FE were resolved clearly.

III. T_C AS A FUNCTION OF STRESS: DETERMINATION OF THE INFINITE-STRESS LIMIT

We now discuss the stress dependence of the critical temperature $T_c(\vec{S})$ in the several directions, and we use these results to provide a new method for determining experimentally when infinite-stress conditions effectively have been reached. By infinite stress we mean in the case of electrons a stress sufficiently high that the splitting between the electron bands is larger than the electron Fermi energy and also large enough to permit a fast thermalization between nondegenerate conduction bands via intervalley phonons.[11] In the case of holes this means that the holes occupy a single band with an effective parabolic dispersion (energy-independent

mass) for energies up to the hole Fermi energy.

The stress dependence of the valence band is somewhat more complex than that given by simply considering the number of bands occupied. The theoretical work of Liu[18] and of Kirczenow and Singwi[31] demonstrates that even if the topmost ($|m_j| = \frac{1}{2}$) valence band is occupied by holes the corresponding density of states can be considerably higher than in the high-stress case. The enhancement of the density of states of the holes is due to valence-band nonparabolicity at low stresses and is caused by the coupling of the $|m_j| = \frac{1}{2}$ band with the $|m_j| = \frac{3}{2}$ band. Even in the case when the valence-band splitting is much larger than the Fermi energy of the holes no true high-stress limit is expected. If the valence-band splitting becomes comparable to the difference in energy Δ between the top of the valence band in the unstressed case and the top of the split-off band [$\Delta = 44.1$ meV (Ref. 32)], coupling between the $|m_j| = \frac{1}{2}$ valence band and the split-off band continuously reduces the density-of-states mass of holes with increasing stress.[33]

We have used the stress dependence of the critical temperature $T_c(\vec{S})$ for electron-hole liquid formation as a new experimental method to estimate the amount of stress necessary to approximate the infinite-stress limit. This method has the advantage that it is independent of assumptions about the stress dependence of the band structure. Such models of the stress dependence of the band structure are necessary to calculate the ground-state density[18,31] and the critical temperature[18] and to obtain the EHL density as a function of stress $n(\vec{S})$ (Ref. 34) from experimental data. Our data for $T_c(\vec{S})$ therefore are particularly well suited for investigations at medium-stress values, i.e., to study experimentally the effects of changes in the density of states of electrons and holes. The T_c values depicted in Fig. 4 are determined in a straightforward manner. The critical point is given by the temperature at which the EHL can no longer condense. At T_c the emission intensity due to EHL vanishes. We simply measure the luminescence intensity of the EHL as a function of temperature for different stress values and seek the temperature at which the EHL emission disappears in the background which is less dependent on temperature. The measurements were performed with a spectral resolution of 1 meV at the stress-dependent energy of the EHL intensity maxium. A detection-gate width of $\cong 1$ μs ensured that the thermalized distribution of the electronic system is observed.[35,36]

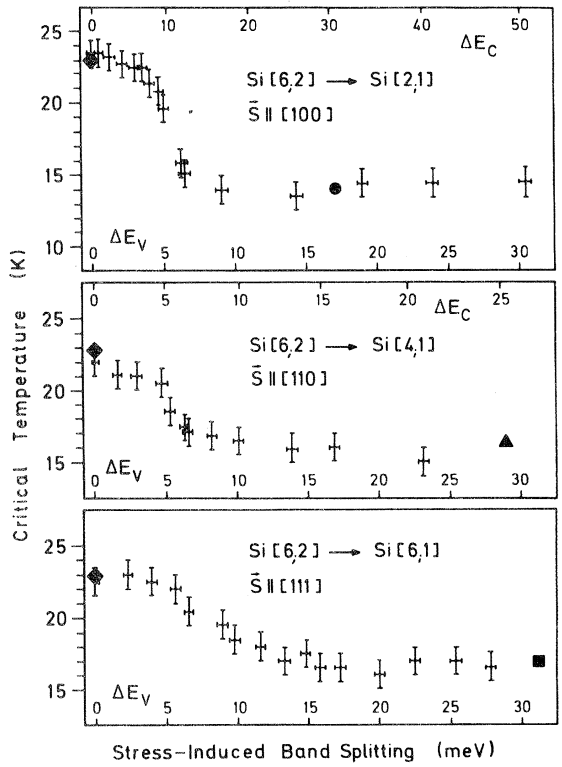

FIG. 4. Experimental data (crosses with error bars) for the critical temperatures measured as a function of stress along the [100], [110], and [111] directions. The stress is represented by the stress-induced conduction- and valence-band splittings. The critical temperatures obtained from measurements of the EHL phase diagrams are also included (solid symbols). For details see text.

In Fig. 4 the critical temperatures for the EHL condensation measured at increasing stress are plotted (crosses with approximate error bars indicated) for stresses along the [100], [110], and [111] axes. On the upper and lower abscissas in Fig. 4 the stress-induced conduction- and valence-band splittings ΔE_c and ΔE_v calculated using the experimentally observed energy shift of the free exciton and the results of stress-dependent absorption measurements of Laude *et al.*[37] are shown. The values of the critical temperatures obtained from the experimental phase diagrams (see Sec. VI) for Si[6;2], Si[2;1], Si[4;1], and Si[6;1] are included (solid symbols) in Fig. 4. These two different methods give nearly identical results for T_c.

All three transitions from unstressed to highly stressed Si display a similar behavior. At small band splittings ($\Delta E_v < 3$ meV) T_c depends only very weakly on stress and roughly equals the un-

stressed value. Then a strong decrease of T_c follows with increasing stress, which is particularly pronounced for $\vec{S}\|$ [100] and $\vec{S}\|$ [110] and somewhat smeared out for $\vec{S}\|$ [111].

Measurements at further increased stress give the same values for the critical temperatures which then depend only on the stress direction. We conclude that for the corresponding stresses the infinite-stress limit effectively is achieved at the critical densities n_c for EHL condensation.

In order to reach infinite-stress conditions for measurements of the complete phase diagrams, especially at lower temperatures (higher densities and higher Fermi energies), stresses higher than those corresponding to the onset of the high-stress regions in the $T_c(S)$ plots are required. Using a scaling relation between the ground-state density and the critical density ($n_c/n_0 \cong 0.3$, Refs. 3 and 22) the ratio of the hole Fermi energy at T_c to the hole Fermi energy in the ground state is estimated to be $\simeq 0.5$. Combining the results of the $T_c(S)$ measurements and this Fermi energy ratio we conclude that in the case of holes in the EHL the infinite-stress limit is reached for valence-band splittings of approximately 14, 18, and 28 meV for Si[2;1], Si[4;1], and Si[6;1], respectively. Infinite-stress conditions for the split conduction bands of Si[2;1] and Si[4;1] require a minimum ΔE_c of $\cong 20$ meV to allow for fast-phonon-assisted intervalley thermalization. In Si[2;1] infinite-stress conditions are reached for electrons and holes at roughly the same stress of $\cong 3$ kbar. In Si[4;1] the conduction-band splitting is a much weaker function of stress than in Si[2;1] and $\Delta E_c \cong 20$ meV is reached for $S \cong 5$ kbar. For the determination of the complete phase diagrams reported below for the systems Si[2;1], Si[4;1], and Si[6;1], stresses of 3.7, 6, and 7 kbar, respectively, were used. These stresses give rise to conduction-band splittings of 30, 25, and 0 meV and valence-band splittings of 17, 29, and 31 meV. As discussed above these splittings should be large enough to realize effectively the infinite-stress limit for all directions of stress.

The general features of $T_c(\vec{S})$ can be understood on the basis of variations of band structure with stress. For Si[2;1] and Si[4;1] the most pronounced effect of stress upon the critical temperature results from the simultaneous decrease in effective conduction-band degeneracy and the reduction of the density-of-states mass of holes. Both effects occur within the same small stress interval. Therefore only a single step in the $T_c(\vec{S})$ curves is observed. In the transition from Si[6;2] to Si[6;1] only the hole density-of-states mass is changed. From a comparison of the behavior of T_c in the transitions from Si[6;2] to Si[2;1] or to Si[4;1] with that in the transition from Si[6;2] to Si[6;1] we see that high-stress conditions are reached rather abruptly for the conduction bands, but that due to the slow change of the effects of hole-band nonparabolicity with stress, its approach to the high-stress value is slower. Qualitatively similar results have been obtained theoretically[31] and experimentally[34] for the stress dependence of the ground-state density.

IV. EXPERIMENTAL DETERMINATION OF LIQUID AND GAS DENSITIES

In the first part of this section typical luminescence spectra are discussed, emphasizing the systematic changes of the emission bands with varying band structure and varying temperature. In the second part a brief outline of the model line shapes used to calculate the emission curves is given, emphasizing novel features of the present work. The densities of the gas and EHL on the phase diagram are determined by fitting calculated line shapes to the experimental spectra. Special care is used near T_c, where the emission bands of free excitons, electron-hole liquid, and electron-hole plasma form a single poorly structured luminescence band.

Figure 5 displays experimental luminescence spectra (circles) for the three stress configurations Si[2;1], Si[4;1], and Si[6;1] together with spectra of unstressed Si[6;2]. For each band configuration a low-temperature spectrum ($T_{\mathrm{EHL}} \cong 0.3T_c$), an intermediate-temperature spectrum ($T_{\mathrm{EHL}} \cong 0.7T_c$), and a spectrum obtained at about $1.2T_c$ are shown. In all cases the temperatures correspond to those of the electronic systems and have been obtained from fits to the spectra. The solid lines give the fit in terms of emissions from electron-hole liquid (EHL), electron-hole plasma (EHP), biexcitons (BI), and free excitons (FE) as discussed below. Figure 5 demonstrates that, independent of the wide band structure variations, the spectra develop in a similar way with temperature for T scaled to each T_c. At low temperatures EHL and FE luminescence are separated clearly. For temperatures between $\cong 0.6T_c$ and the critical point the overlapping emissions of EHL, EHP, and FE lead to a single

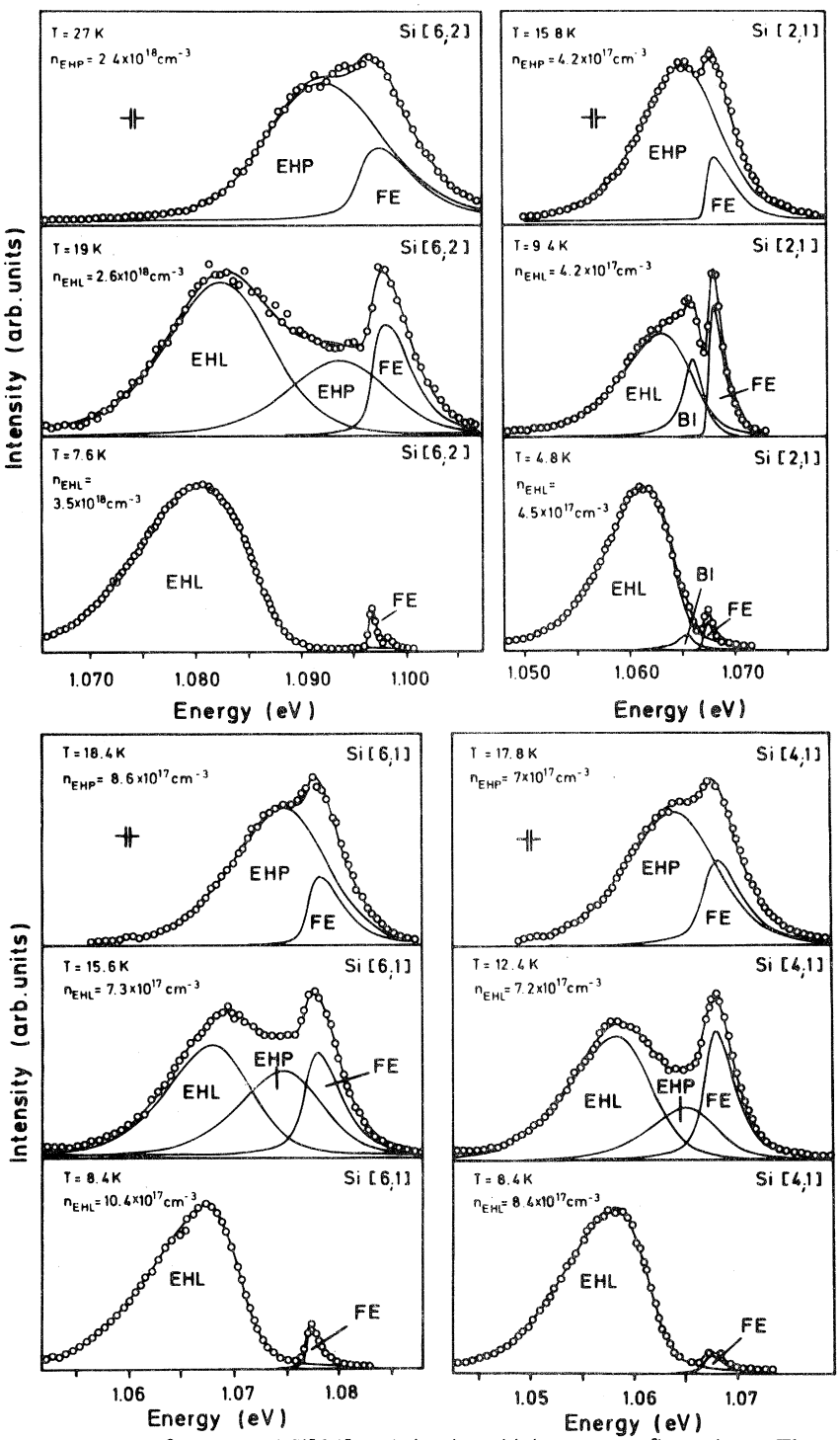

FIG. 5. Luminescence spectra of unstressed Si[6;2] and the three high-stress configurations. These spectra were obtained at temperatures $\cong 0.3T_c$, $0.7T_c$, and $1.2T_c$, respectively. The experimental data points have been fitted with theoretical line shapes for EHL, EHP, BI, and FE (solid lines).

poorly structured emission band. At the critical temperature this broad band narrows distinctly within a temperature interval of ~ 1 K. Above T_c only EHP and FE contribute to the luminescence.

In order to obtain reliable results for the EHL density as a function of temperature in the important region near the critical point the origin of all overlapping luminescence emissions must be known

accurately. Recently, the luminescence band situated between EHL and FE has been discussed using two different models: (i) this emission has been attributed to higher-order bound states, e.g., biexcitons and trions,[13,38] or (ii) it has been assigned to the emission from a dense electron-hole plasma.[15,39,40]

We adopt the latter interpretation for the following reasons. The EHP spectra recorded slightly above T_c have a linewidth and a line shape which varies between the Si systems with the density-of-states mass in the same way as the linewidth and the line shape of the EHL itself (Fig. 5). Variations of the linewidth and the line shape of the emissions from higher-order bound states, on the other hand, would be determined by the optical mass, which remains the same in all four Si band configurations.[16] Therefore we exclude them as an explanation for this emission. Also, it has been reported[40] that a characteristic feature of the EHP is a very weak dependence of the EHP density on the excitation level. Thus at first glance it might be tempting to interpret the EHP as a high-temperature EHL. A similar point has been made by Thomas *et al.*[13] for Ge. We have been able to make a clear distinction between EHL and EHP from careful analyses of spectra recorded over a wide range of temperatures ($T < 50$ K). EHP and EHL can be distinguished by the comparison of the respective temperature dependence of the density. The density of the EHL decreases if T is increased.[3] In contrast, the EHP density increases with increasing temperature.[40]

Owing to the rather poorly structured emission bands in the particularly interesting temperature region around the critical point careful numerical line-shape analyses were necessary in order to obtain reliable values for the electron-hole liquid density n_{EHL} and for the temperature-dependent work function of the excitons (which has been used to give estimates of the gas density, see below). The theoretical line shapes have been calculated as follows.

(1) The line shape of free excitons is obtained following Elliott's theory[41] assuming parabolic bands and a Boltzmann distribution. In the present work consideration of the overlapping TO-LO replicas of the luminescence emissions has been included. Both levels of the split exciton ground state have been included to account for the temperature-dependent TO-LO intensity ratio at zero stress.[42] The high-stress value of the TO-LO intensity ratio ($R_{\mathrm{TL}} = I_{\mathrm{TO}}/I_{\mathrm{LO}}$) differs from that of unstressed Si. From fits to low-temperature emission spectra of free excitons we obtain $R_{\mathrm{TL}} \cong 17$ instead of the low-temperature zero-stress value of $\cong 2$.[42] Merle *et al.*[43] have shown experimentally that the transition observed in emission spectroscopy at high stresses starts from the Δ_6 level of the exciton ground state. Using careful line-shape fits to the FE emission, Hammond and Silver[42] have determined for the Δ_6 level a value of $R_{\mathrm{TL}} \cong 15$, which is in good agreement with our data. Unlike the unstressed case, the high-stress value of the TO-LO intensity ratio shows no temperature dependence. Owing to the large valence-band splitting compared to the thermal energy, only the lowest excitonic state is occupied even at high temperatures.

(2) The biexciton line shape was calculated following Cho's theory.[44] From different spectra recorded at low temperatures and at weak excitation intensities we determine the broadening parameter $\Gamma = 0.8$ meV in agreement with the results of Thewalt and Rostworowski.[45] We obtain a BI binding energy $E_{\mathrm{BI}} = 1.45 \pm 0.05$ meV for all Si band configurations.[46,47] This result is in agreement with Si[2;1] results of Gourley and Wolfe[48] and with a Si[6;2] value given by Thewalt *et al.*,[49] but it differs distinctly from $E_{\mathrm{BI}} = 0.5$ meV reported by Kulakowskii *et al.*[10]

(3) Special care was taken in calculating the line shapes of the electron-hole liquid and electron-hole plasma emissions. The standard convolution of the densities of states of electrons and holes, which is used to describe the EHL emission line shape has been improved significantly by inclusion of a broadening due to intravalley scattering[50] and by the use of Fermi energies which are calculated numerically from the Fermi integrals. We see that there are significant differences, particularly in the region of the reduced band gap, when we compare the experimental line shapes with those given by a simple fit which is based on the usual unbroadened convolution of the densities of states. Martin and Störmer[51] and Schmid[52] have demonstrated that a model proposed by Landsberg,[50] which involves an energy-dependent broadening function of the density of states of electrons and holes due to the finite intraband relaxation times, can account for these differences. The broadening used here is based on a generalization to nonzero temperature of the original $T = 0$ K model, and includes lifetime broadening of states above the Fermi level.[53] The use of this broadening function leads to excellent agreement between experimental and theoretical

line shapes (see Fig. 5) which is essential for a reliable evaluation of the densities on the phase diagrams, particularly in the high-temperature range.

In the present fits for the contribution of EHL and EHP to the line shapes we assume only charge neutrality and parabolic densities of states for electrons and holes. The Fermi energies and hence the EHL densities as functions of temperature are then evaluated by direct numerical integration over the Fermi distributions. The high-stress density of states masses reported by Hensel and Feher[17] listed in Table I are used. This procedure is necessary in several cases of high stress for which the usual T^2 expansion of the electron Fermi energy E_F breaks down. For example, for Si[6;1], $E_{FE} \cong 1.9$ meV at 16 K which is comparable to the thermal energy.

The densities of the liquid phase and the coexisting gas phase on the phase diagram are obtained from fits of the luminescence bands as the appropriate sum of EHL, EHP, BI, and FE line shapes as follows:

(1) The liquid density is related to the width and shape of the EHL component, and the EHL density on the coexistence curve is obtained directly from the detailed line-shape fits.

(2) Some additional analysis is required to obtain the gas densities from the data because a direct, absolute method to measure the gas densities is not available (see discussion below). Along the coexistence curve the gas is pictured in terms of noninteracting components of free excitons, electrons and holes, and higher-order complexes formed by them. The densities of the gas constituents in equilibrium with the liquid can then be calculated from Richardson-type equations[13,54]:

$$n_i(T) = l_i g_i \left[\frac{m_i k_B T}{2\pi\hbar^2} \right]^{3/2} \exp\left[\frac{-\phi_i}{k_B T} \right] . \quad (1)$$

Here l_i denotes the number of electron-hole pairs of the gas species,[13] g_i the degeneracy factor (Table II), m_i its translational mass, and ϕ_i its work function. For these calculations a parabolic dispersion has been assumed for each component. The values of g_i, m_i, and ϕ_i are subject to some uncertainty,

TABLE II. Degeneracy factors of free excitons and biexcitons in Si.

	Si[6;2]	Si[6;1]	Si[4;1]	Si[2;1]
g_{ex}	24	12	8	4
g_{BI}	66	66	28	6

and to our knowledge detailed calculations for them are not available to date. For the mass of the free exciton in Eq. (1) we use a value of $0.5m_0$.[55] An averaged mass of $0.25m_0$ is used for electrons and holes. The work function ϕ_i of the different gas species is approximated from several parameters, which include the number of electron-hole pairs l_i which form the complex, the exciton work function ϕ_{FE}, the exciton binding energy E_{ex}, and the binding energy of the complex (with respect to the FE) E_B. This gives

$$\phi_i = l_i(1-\alpha)\phi_{FE} + \alpha E_{ex} - E_B , \quad (2)$$

where $\alpha = 0.5$ for charged complexes and $\alpha = 0$ for neutral complexes. The temperature-dependent work function of the free excitons ϕ_{FE} is obtained by fitting the difference between the bottom of the free exciton band and the chemical potential of the liquid. A binding energy $E_B = 1.45$ meV has been used for biexcitons and an equal value for trions. We consider only these two small complexes because higher-order complexes have larger work functions [Eq. (2)]. Hence their contributions to the gas density $n_g = \sum n_i$ can be neglected. From Eqs. (1) and (2) the largest contributions of complexes to the gas phase are expected in the case of Si[2;1], where ϕ_{FE} and E_B are comparable. The biexciton densities roughly equal the free exciton densities in thermal equilibrium with the EHL. This is the reason for comparable emission intensities of BI and FE in this band structure (Fig. 5).[46]

For all four Si band configurations the resulting gas densities $n_g(T)$ are plotted as a function of

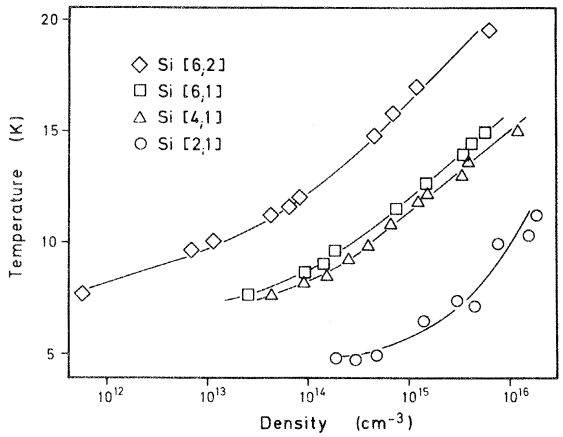

FIG. 6. Experimental densities of the gas phase in equilibrium with EHL as a function of temperature in the four Si band configurations.

temperature in Fig. 6. Owing to the large differences in the exciton work functions of the different Si systems (Table VI) large variations of the gas densities are found between the systems.

The basic assumption of an ideal gas in thermal equilibrium with the liquid is approximately valid at intermediate temperatures $0.2T_c \leq T \leq 0.8T_c$. It breaks down at low temperatures due to supersaturation effects[56] and at high temperatures and high densities due to increasing interactions.[13]

In addition to the present method for estimating the gas densities, other proposals have been made previously to obtain $n_g(T)$.[3,12,57] Thomas *et al.*[57] have shown that exciton-exciton scattering leads to a density-dependent broadening of the FE line. Unfortunately a separation of this comparatively weak effect from the overlapping EHP or BI emission cannot be performed with sufficient accuracy to permit reliable estimates of the exciton density. Onset measurements[3,12] in which exciton densities are determined from the onset of EHL luminescence as the temperature is lowered at a fixed excitation intensity are also unsatisfactory. They require a temperature-independent carrier lifetime and diffusion length in contradiction with experimental results.[30,47] Furthermore the relative exciton densities have to be calibrated at T_c where the flat top of the phase diagram might introduce substantial errors. In view of the large uncertainties in the latter methods we believe that the most reasonable estimates for the gas densities are obtained from the Richardson equations described above.

V. THEORETICAL APPROACHES AND RESULTS

In this section the results of microscopic calculations of the ground-state properties and of the critical points for EHL in the four Si systems under effectively infinite-stress conditions are given. The theoretical approaches used to calculate critical points also are reviewed briefly.

The ground-state energy E_0 and density n_0 are calculated in the usual way from the minimum of the energy versus density n of a dense EHL:

$$E(n)=E^k(n)+E^{xc}(n) . \tag{3}$$

The results are given in Table III. The kinetic energy $E^k(n)$ was obtained exactly. For Si[6;2] and Si[2;1] the exact exchange energy was used, and also the detailed results for the correlation energy obtained by Vashishta *et al.*[58] were used. For Si[6;1] and Si[4;1] detailed calculations of the correlation energy are not yet available. It has been noted,[22,59,60] however, that the combined exchange-correlation energy $E^{xc}(n)$ when expressed in appropriate atomic units is quite insensitive to the degeneracy and anisotropy of the band structure. The results for these two systems given in Table III were obtained using the average of the $E^{xc}(n)$ for all six Ge and Si systems for which detailed calculations have been made. Corresponding calculations for Si[6;1] and Si[4;1] have also been made using $E^{xc}(n)$ appropriate for the different individual systems, and only small changes were found [$\leq 3\%$ for n_0 and $\leq 4\%$ for $E(n_0)$]. It might be noted that the values of n_0 for both Si[6;1] and Si[4;1] obtained using $E^{xc}(n)$ for Si[2;1] (which represents best the nondegenerate hole band) are approximately 3% larger than the values using the average $E^{xc}(n)$ above.

The temperature dependence of the EHL density at low temperatures is obtained from the minimum of the free energy per pair $F(n,T)$ as a function of density n where $F(n,T)$ is expanded to lowest order in k_BT/E_{Fi}:

$$F(n,T)\cong(n)-\tfrac{1}{2}\gamma(n)(k_BT)^2 , \tag{4}$$

$$\gamma(n)=\hbar^{-2}(\pi/3)^{2/3}\mu_0^{-1}(m_{de}+m_{dh})n^{-2/3} , \tag{5}$$

where μ_0 is the reduced optical mass.

In Eq. (4) the usual[3,4] approximations have been used. $E^{xc}(n)$ has been taken to be temperature independent and bare masses are used in $\gamma(n)$. These are good approximations because the effects of

TABLE III. Calculated values for the ground-state density n_0, the exciton work function ϕ_0, the ground-state energy E_0, and the liquid expansion coefficient at low temperatures δ_n. For details of the calculation see text.

	Si[6;2]	Si[6;1]	Si[4;1]	Si[2;1]
n_0 (10^{18} cm^{-3})	3.25	0.833	0.696	0.451
ϕ_0 (meV)	7.4	3.8	3.0	1.95
E_0 (meV)	−22.1	−16.6	−15.8	−14.75
δ_n (10^{-3} K^{-2})	0.767	1.82	1.66	1.82

exchange-correlation have been found[3,4] to lower the bands nearly rigidly. The resulting EHL density has a quadratic variation with T given by $n(T)=n_0(1-\delta_n T^2)$, and the low-temperature liquid expansion coefficients δ_n calculated here for the present systems are also given in Table III.

Two approaches have been proposed to treat aspects of the properties of EHL at higher temperatures. These are the uniform-plasma approach for the critical point and the droplet-fluctuation approach for the phase diagram including the critical point. In the uniform-plasma approach the chemical potential $\mu(n,T)$ of a uniform electron-hole liquid system is considered as function of density n for various temperatures T. The critical point is given by an inflection point in the chemical potential versus density. Combescot[23] has pointed out that the critical point for EHL generally occurs where the system remains approximately dense and degenerate, and therefore a simple free energy like that in Eq. (4) can be used. Recently Reinecke *et al.*[26] have pointed out that this approach gives a reliable upper bound for T_c which is not unduly sensitive to the treatment of the correlation energy; in principle, however, this approach overestimates T_c because it neglects statistical fluctuations in the critical region. In Table IV the values of T_c and n_c obtained from the uniform-plasma approach using the free energy in Eq. (4) are given for the present systems.[61]

The droplet-fluctuation approach for EHL condensation has described successfully the entire phase diagram including the critical point.[25,26] It is based on a picture of the gas near condensation as a series of noninteracting dropletlike fluctuations and of the liquid as a dense EHL containing bubblelike fluctuations of the gas phase. The densities on the gas and liquid sides of the condensation phase diagrams are given by[25,26]

$$n_{G,\mathrm{coex}}=q_0\sum_l l^{1-\tau}\exp\left[\frac{-\sigma(T)al^\eta}{k_BT}\right], \tag{6a}$$

$$n_{L,\mathrm{coex}}=n(T)-q_0\sum_l l^{1-\tau}\exp\left[\frac{-\sigma(T)al^\eta}{k_BT}\right]. \tag{6b}$$

Here $\sigma(T)$ is the temperature-dependent surface tension, and $n(T)$ is the variation of the EHL density due to single-particle excitations defined above, $q_0=n_c/\zeta(\tau-1)$, $\zeta(x)$ is the Riemann ζ function, $\tau\cong 2.2$, and al^η ($\eta=\frac{2}{3}$) is the droplet surface area. In this approach the critical point is given by the temperature for which the droplet surface tension vanishes $\sigma(T=T_c)=0$, and stable droplets can no longer form. The corresponding critical density is $n_c=\frac{1}{2}n_0(1-\delta_n T_c^2)$. The phase diagram is expressed in terms of the quantities $\sigma(T)$ and $n(T)$ characterizing the low-temperature EHL which can be expanded:

$$\sigma(T)\cong\sigma_0(1-\delta_\sigma T^2), \tag{7}$$

$$n(T)\cong n_0(1-\delta_n T^2). \tag{8}$$

Thus the phase diagram is expressed in terms of four parameters σ_0, $T_c(=\delta_\sigma^{-1/2})$, n_0, and δ_n.

The droplet fluctuation approach can be used in two rather different ways: (1) experimental data can be fitted to obtain values of these parameters[62]; (2) theoretical phase diagrams can be formed from microscopic calculations of the parameters. In particular, a method for calculating the temperature-dependent surface tension based on the free energy as a functional of the density has been developed.[26,63] Results for the critical points of the four Si systems studied here using this method are given in Table V.

VI. COMPARISON OF EXPERIMENT AND THEORY; DISCUSSION

Here we describe how the ground-state and critical parameters are obtained from measurements of the phase diagrams for the four systems. In particular, it should be noted that the critical points are obtained by fitting data for the phase diagram away from the critical region with the form given by the droplet-fluctuation model, and thus difficulties associated with fitting spectra in the immediate vicinity of the critical point are avoided. In this section we also discuss the important impli-

TABLE IV. Critical temperature and critical density of unstressed Si and Si under high uniaxial stress calculated on the basis of the uniform-plasma model for the critical point.

	Si[6;2]	Si[6;1]	Si[4;1]	Si[2;1]
T_c (K)	29.0	21.4	20.8	17.4
n_c (10^{18} cm^{-3})	0.412	0.1308	0.112	0.0748

TABLE V. Values for the critical temperature, critical density, and zero-temperature surface tension σ_0 obtained from microscopic calculations within the droplet-fluctuation approach.

	Si[6;2]	Si[6;1]	Si[4;1]	Si[2;1]
T_c (K)	23.3	16.5	15.8	14.1
n_c (10^{18} cm^{-3})	0.951	0.210	0.204	0.144
σ_0 (10^{-4} erg/cm^2)	35.0	7.79	6.40	3.73

cations of the present experimental results for proposed scaling relations between the ground-state and critical parameters and also for theoretical models of the critical point.

As described in Sec. IV, the coexisting densities of the gas and the liquid have been determined as a function of temperature from numerical line-shape fits to luminescence spectra of the four different Si systems. All experimental phase diagrams are shown in Fig. 7(a), and the phase diagrams for the three high-stress configurations are plotted on an enlarged scale in Fig. 7(b). The phase diagrams show substantial changes with varying band structure in the present systems. The most pronounced effects occur for the ground-state densities which are reduced by approximately a factor of 8 in going from unstressed Si to Si under high stress along the [100] direction. The critical temperatures are somewhat weaker functions of the band configuration.

We fitted the experimental data for the phase diagrams with the corresponding equations (6)—(8) from the droplet-fluctuation model, in which the low-temperature parameters (n_0,δ_n,σ_0) and critical temperature T_c were adjustable.[62] For these fits only data from the liquid side of the coexistence curves were used because of the uncertainties in the experimental determination of the gas densities.

The use of phase-diagram fits to obtain the characteristic parameters of the electron-hole liquid is necessary because of the following.

(1) Measurements at $T \cong 0$ K or sufficiently low T which would give the ground-state parameters directly cannot be performed. From line-shape fits we find EHL temperatures of $\cong 4.5$ K for bath temperatures of 1.7 K. Two mechanisms might be responsible for this effect: heating of the EHL by Auger electrons and holes and sample heating by the high excitation intensities.

(2) In the particularly interesting temperature range around T_c the EHL emission intensity decreases drastically with increasing temperature,

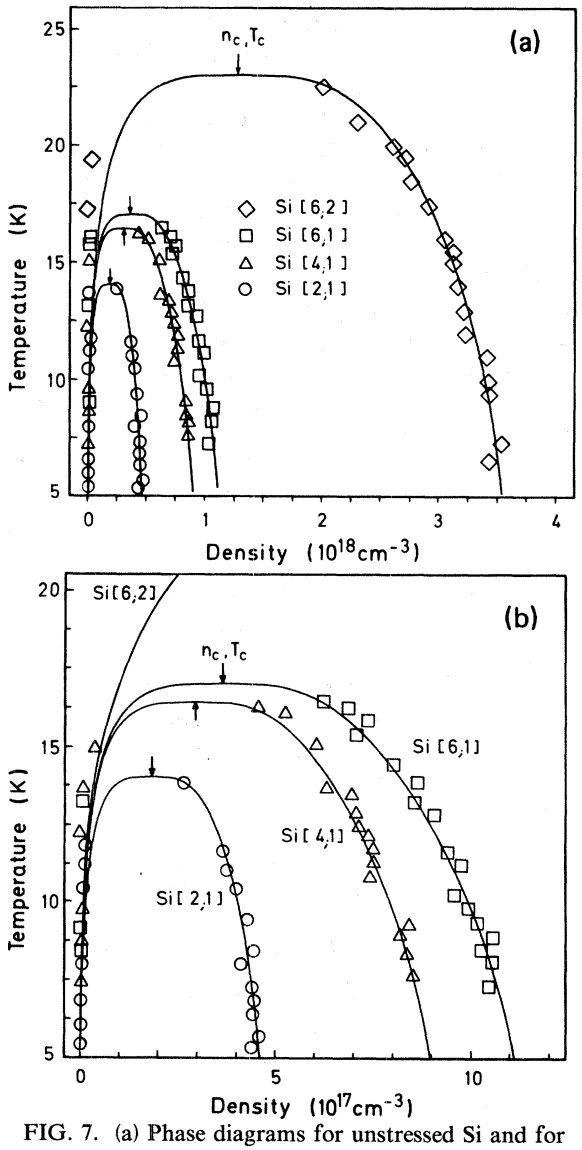

FIG. 7. (a) Phase diagrams for unstressed Si and for Si under high uniaxial stress in the [111], [110], and [100] directions. Included are fitted phase diagrams which are calculated following the droplet-fluctuation approach and which give the experimental values for the ground-state and critical parameters. (b) Details of the phase diagrams of uniaxially stressed Si.

whereas the EHP emission intensity increases in this temperature region. Hence line-shape fits to the overlapping emission of EHL, EHP, and FE become somewhat insensitive to the EHL parameters.

The ground state and critical parameters can be extrapolated accurately from phase-diagram fits using the experimental data in the temperature range $0.3T_c \leq T_{\mathrm{EHL}} \leq 0.95T_c$. The results for these parameters are given in Table VI. Using this approach the different uncertainties for the various quantities arise from their different sensitivities to features of the phase diagrams. In these fits the ground-state density and the critical temperature are independent parameters and are determined with the least uncertainty. The low-temperature liquid expansion coefficient δ_n, the surface energy σ_0, and the critical density n_c depend on each other, and larger uncertainties are found for them: A larger value of δ_n has a somewhat similar effect on the shape of the phase diagram as does a smaller value for σ_0, and it reduces the critical density. It should be noted that the values of the critical temperatures obtained by the present procedure are in good agreement with those obtained by onset measurements (see Fig. 4).

The experimental data for the ground-state energy

$$E_0(n_0) = -[\phi_0(n_0) + E_{\mathrm{ex}}] \tag{9}$$

were obtained from the low-temperature values of $\phi(n(T))$ in which the leading influence of the temperature ($\sim T^2$) was corrected.[4,64] A value of 14.7 meV (Ref. 65) was used for the exciton binding energy E_{ex} in the case of Si[6;2].[66] For the simple band structures of the high-stress systems E_{ex} is approximated rather accurately by the exciton Rydberg (= 12.85 meV).[4,29]

The present experimental value for the ground-state density in unstressed Si is comparable to (although somewhat higher than) previous results of Hammond *et al.*[8] (3.33×10^{18} cm^{-3}) and Dite *et al.*[14] (3.35×10^{18} cm^{-3}). The differences arise from the neglect of intravalley relaxation broadening in Refs. 8 and 14.[52] Recent data of Kulakovskii *et al.*[10] and of Schmid[52] who include relaxation effects in their line-shape fits give 3.5×10^{18} cm^{-3}, in good agreement with the present value.

A more important difference is found between the present value of the critical temperature $T_c \cong 23$ K for Si[6;2] and those previously reported which are $T_c \cong 28$ K (Ref. 14) and $T_c \cong 27$ K (Ref. 15). A comparison of experimental spectra published by Dite *et al.*[14] with those given by Shah *et al.*[15] shows, that although the T_c values given by them are very similar the temperature scales are different. For example, in Ref. 14 a spectrum which displays EHL, EHP, and FE emissions has been assigned an EHL temperature of 25 K. We would give a temperature $T \cong 20$ K to this spectrum. We attribute this difference in temperature assignments to the lack of line-shape fits of the complete high-temperature emission bands in Ref. 14. Shah *et al.*,[15] on the other hand, assign approximately the same temperatures to their spectra as we do. They, however, have not made detailed fits to the luminescence spectra considering contributions from FE, BI, EHP, and EHL as is done in the present work. This leads them to describe spectra at temperatures $\gtrsim 23$ K in terms of FE and EHL rather than FE and EHP, and thus it results in their overestimate of T_c.

For the high-stress configurations few experimental data have been reported to date.[67] Kulakovskii *et al.*[10] give 0.98×10^{18} cm^{-3} for the

TABLE VI. Experimental results for the ground-state and critical parameters in unstressed Si and in Si under high uniaxial stress. The values for n_0, δ_n, σ_0, T_c, and n_c have been obtained from fits of the experimental phase diagrams with model curves calculated from the droplet-fluctuation model (Fig. 7). For the determination of the ground-state energy and the exciton work function see text.

	Si[6;2]	Si[6;1]	Si[4;1]	Si[2;1]
n_0 (10^{18} cm^{-3})	3.6 ±0.1	1.15±0.02	0.93±0.02	0.475±0.01
δ_n (10^{-3} K^{-2})	0.53±0.1	1.3 ±0.2	1.4 ±0.2	1.4 ±0.2
ϕ_0 (meV)	9.3 ±0.2	5.4 ±0.2	4.9 ±0.2	2.2 ±0.2
E_0 (meV)	−24.0 ±0.2	−18.2 ±0.2	−17.7 ±0.2	−15.0 ±0.2
σ_0 (10^{-4} erg/cm^2)	28 ±5	10 ±3	8 ±3	4 ±2
T_c (K)	23.0 ±1.0	16.9 ±0.5	16.4 ±0.5	14.0 ±0.5
n_c (10^{18} cm^{-3})	1.2 ±0.2	0.36±0.08	0.29±0.06	0.18 ±0.03

EHL density in Si[6;1], 0.90×10^{18} cm^{-3} for Si[4;1], and 0.48×10^{18} cm^{-3} for Si[2;1]. Their results tend to be lower than our values, which might result from the fact that they give data for low but nonzero temperatures, whereas ours has been corrected to zero temperature using the phase-diagram fits. Wagner and Sauer[11] obtained low-temperature EHL densities of 1.0×10^{18} cm^{-3} and of 0.60×10^{18} cm^{-3} for Si[6;1] and Si[2;1], respectively. Their Si[2;1] value is larger than ours because they did not include a biexciton contribution in the fits of the high-stress spectra. Very recently Kulakovskii *et al.*[68] have published a value for the critical temperature in the case of Si[2;1], which is $T_c\cong14\pm1.5$ K in good agreement with our result.

Our experimental and theoretical results (Tables III and VI) for the ground-state energy and density are in good agreement in the cases of Si[6;2] and Si[2;1], but some differences are found for Si[6;1] and Si[4;1]. These differences might result from residual valence-band nonparabolicities[18,31] which in these cases might tend to increase n_0 somewhat above the infinite-stress value considered in the theory. They might also arise in part from the lack of detailed calculations for the correlation energies for these systems. For the theoretical results we have assumed that the combined exchange-correlation energy E^{xc} is independent of band structure; n_0 might be sensitive to this choice because $E_0(n)$ has a rather flat minimum at n_0.

The systematic trends of the ground-state properties between these systems can be understood on the basis of varying band structure. Since E^{xc} is approximately independent of band structure, the kinetic energy E^k gives rise to the observed stress dependence of the EHL properties. E^k is proportional to the inverse of the density-of-states mass of electrons and holes. For all of the band structures which we investigated m_{dh} is smaller by more than a factor of $\cong2$ than m_{de}. Hence, in unstressed Si and in its high-stress configurations the EHL parameters are determined mainly by the density-of-states masses of the holes. In particular, this leads to the very similar properties for Si[4;1] and Si[6;1] where $m_{de}\cong3m_{dh}$ and $\cong4m_{dh}$ (Table I), respectively [Fig. 7(b) and Tables III–VI].

The present results represent the first detailed experimental study of EHL condensation for a set of systems with widely varying band structure (varying basic energetics). Therefore, for the first time, we are able to test quantitatively certain basic principles for EHL condensation. The most important of these is the idea of general "scaling relations" which have been proposed to exist between the ground-state and critical parameters for EHL condensation independent of system. There has been a persistent search for such relations. A knowledge of such relations would be useful in the investigation of EHL in new materials where it would permit estimates of the critical parameters to be made using the relatively more accessible and accurate EHL ground-state data. Furthermore, scaling relations for EHL are of interest in principle because they can provide insight into the basic physics of the condensation process which can be somewhat hidden by more detailed theoretical calculations.

Several proposals for scaling relations have been made. From the "principle of corresponding states" the relation $\phi_0/k_BT_c\cong$const was suggested.[3] Based on the results of early experiments, the relation $T_c/n_0^{1/2}\cong$const (Refs. 3 and 21) and $n_c/n_0\cong$const (Ref. 3) have been suggested. These relations, however, were not derived from a microscopic theory of EHL condensation. Recently, Reinecke and Ying[22] have given an alternate set of scaling relations. These were based on theoretical studies of the band structure systematics of EHL condensation, and their origin was obtained from the basic energetics of EHL. These relations are

$$\frac{\kappa T_c}{n_0^{1/4}}\left[\frac{\kappa}{\mu_0}\right]^{1/4}\cong\text{const}\ , \tag{10}$$

$$|E_0|/k_BT_c\cong\text{const}\ , \tag{11}$$

$$n_c/n_0\cong\text{const}\ , \tag{12}$$

where κ is the static dielectric constant.

As can be seen from Table VII(a) the first two ratios display a strong band-structure dependence and hence cannot be used as scaling relations. The scaling relations, Eqs. (10), (11), and (12), are satisfied remarkably well. The ratio of the ground-state energy to the critical temperature, Eq. (11), and the relation between the critical temperature and the fourth root of the ground-state density, Eq. (10), are seen to be largely insensitive to band-structure variations. Variations of $\cong10\%$ are found for the ratio n_c/n_0; variations in this ratio are larger than for the others because n_c can be determined with relatively less accuracy than the other parameters. Note that physically the critical temperature is related to $|E_0|$ rather than to ϕ_0 because the EHL condensation occurs from a dense electron-hole plasma rather than from excitons.[22] Also in Eq. (10) the power of the density to which T_c is related arises from the density dependence of

TABLE VII. Scaling relations between ground-state and critical parameters of electron-hole liquid in Si obtained from (a) present experimental values, and (b) theoretical results from the droplet-fluctuation model.

	Si[6;2]	Si[6;1]	Si[4;1]	Si[2;1]
(a) experiment				
ϕ_0/k_BT_c	4.7	3.7	3.5	1.8
$T_c/n_0^{1/2}$ (10^{-9} K cm$^{3/2}$)	12.1	15.8	17.0	20.3
$\frac{\kappa T_c}{n_0^{1/4}}\left[\frac{\kappa}{\mu_0}\right]^{1/4}$ (10^{-2} K cm$^{3/4}$)	1.85	1.81	1.85	1.87
n_c/n_0	0.34	0.32	0.31	0.36
$\lvert E_0\rvert/k_BT_c$	12.1	12.5	12.6	12.5
(b) theory				
ϕ_0/k_BT_c	3.7	2.6	2.2	1.6
$T_c/n_0^{1/2}$ (10^{-9} K cm$^{3/2}$)	12.9	18.1	18.9	21.0
$\frac{\kappa T_c}{n_0^{1/4}}\left[\frac{\kappa}{\mu_0}\right]^{1/4}$ (10^{-2} K cm$^{3/4}$)	1.92	1.91	1.92	1.91
n_c/n_0	0.29	0.25	0.29	0.32
$\lvert E_0\rvert/k_BT_c$	11.0	11.7	11.6	12.1

the exchange-correlation energy ($\sim n_0^{1/4}$) (Ref. 22).

Corresponding results for the scaling ratios obtained from the present calculations of the ground states and of the critical points are shown in Table VII(b), and they are seen to be in good agreement with the experimental values. We note, in addition, that the present values of the scaling relations are in good agreement with those obtained from experiment for Ge, which is the only system for which detailed experimental values have been available previously.[12,13] For Ge, $|E_0|/k_BT_c = 10.3\pm0.7$, $n_c/n_0 = 0.31\pm0.07$, and $(\kappa T_c/n_0^{1/4})(\kappa/\mu_0)^{1/4} = (2.01\pm0.2)\times10^{-2}$ K cm$^{3/4}$. The values of κ and μ_0 vary substantially between Ge and the present Si systems. For Ge (Ref. 4) $\kappa=15.36$ and $\mu_0=0.046$, and for the Si systems,[4] $\kappa=11.4$ and $\mu_0=0.128$. Thus from the last value above, we see that these parameters are correctly included in the form of Eq. (10).

The present experimental results can be used also to discuss two theoretical approaches to the critical point. The experimental values for T_c and the results calculated from the droplet-fluctuation model are in remarkably good agreement for all band configurations (Tables V and VI). If we compare the experimental data to the results of the uniform-plasma approach (Table IV), we find that this model gives reasonable estimates of T_c which are consistently higher by $\cong 20\%$ than the experimental data. Physically this difference between the droplet-fluctuation model and the uniform-plasma model is related to the different picture in which these models describe the critical point. In the uniform-plasma model even at T_c the system is treated as dense and homogeneous. Density fluctuations, which become important as the critical point is approached, are neglected. In the droplet-fluctuation approach, on the other hand, these fluctuations are included in an approximate way, and they are found to lower the critical temperatures. The experimental values for the critical densities n_c are in reasonable agreement with the corresponding results from the droplet-fluctuation approach. From the uniform-plasma model we obtain values of n_c which are consistently lower by a factor of $\cong 3$ than those observed experimentally. These low values of n_c from the uniform-plasma model arise from the fact that its estimates of T_c are high and thus the corresponding values of the density are low.

VII. CONCLUSIONS AND SUMMARY

We have presented the most extensive study to date of electron-hole liquid systematics using unstressed Si and Si subject to high uniaxial stress.

The use of these four band configurations enables us to study EHL formation in a clearly defined set of widely varying band structures. Based on experimental and theoretical results for the phase diagrams, the ground states, and the critical parameters, general trends for electron-hole liquid condensation have been obtained.

The present experimental results for the electron-hole liquid ground states and critical points have been used to test and to verify recently proposed scaling relations. From these tests the correct forms of several of these relations have been obtained. Our results for the critical points have been used to distinguish between the uniform-plasma model and the droplet-fluctuation model. Both are found to give reasonable values for T_c but the neglect of fluctuations in the liquid near the critical point which is made by the plasma model leads to consistent overestimates of T_c. The critical points obtained from the droplet-fluctuation model are in remarkably good agreement with the experimental results.

Note added in proof

After the submission of the present manuscript we became aware of the results of recent studies by Gourley and Wolfe [P. A. Gourley and J. P. Wolfe, Phys. Rev. B 24, 5970 (1981)] on EHL in a spatially nonuniform strain well created by (100) strain in Si. These authors (GW) report values of n_0 and T_c which differ quantatively from ours for the corresponding case of uniform (100) stress. The relationship between results from such experiments done on strain wells and those with uniform strain is not yet understood in detail, and there are some differences in methods of analysis. We are confident in our results, and we suggest that the spatial confinement and the excitation conditions may result in a somewhat different spatial and temporal thermodynamic character of the electron-hole system in the two systems. We believe that our uniform strain results better represent the uniform equilibrium system to be compared with theory. This view is supported by the facts that our results for the ground state and thermodynamic parameters are in good agreement with theory, that they show the expected variations with changes in band structure, and that the phase diagrams are in accord with the basic properties of Fermi systems. We note these points briefly here.

For n_0 GW obtain 3.5×10^{17} cm^{-3} which is smaller than our value of 4.8×10^{17} cm^{-3} and smaller than recent theoretical values. Part of this difference is accounted for by our inclusion of the effects of linebroadening due to intraband transitions in our line-shape fits ($\sim\frac{1}{3}$ of difference) and by our extrapolation of n_0 to zero temperature. The most striking differences between the two sets of results occur for the thermodynamic and critical properties. GW obtain a phase diagram whose liquid side has no temperature dependence in contradiction to what is expected for Fermi systems with these Fermi energies. GW obtain an estimate of $T_c\approx20$ K which is larger than our value of 14.0 K. Their estimate is obtained from the temperature at which the lower half maximum of a broad luminscence line shifts to higher energy. We use two different procedures for T_c, one based on a fit of the phase diagram formed from detailed line-shape analyses away from T_c, and the second involving onset measurements, and these two methods give results in good agreement with one another. On dimensional grounds the value of T_c reported by GW appears to be larger than expected in comparison with the value for unstrained Si ($\cong23$ K). Their T_c with strain is larger than expected from comparing their ground-state energy and density with those for the unstrained case. More quantitatively, the scaling relationships (Ref. 22) also suggest that their value of T_c is larger than expected. In our studies of a series of systems with no strain and with uniform strains in three directions, we find systematic variations in quantitative agreement with theory and with the scaling relations.

We thank P. L. Gourley and J. P. Wolfe for discussions of our respective results.

ACKNOWLEDGMENTS

We would like to thank M. H. Pilkuhn for stimulating discussions and G. Moersch for expert technical assistance. We are indebted to P. T. Landsberg and D. J. Robbins for deriving a very useful formula for the relaxation broadening in

EHL. Thanks are due to E. Gmelin of the Max-Planck Institut für Festkörperforschung (MPIF), Stuttgart, for his aid in constructing the variable-temperature Dewar and to E. Kisela of the MPIF for the preparation of the samples. One of us (T.L.R.) is grateful for the hospitality of the MPIF during the initial stage of this work. The financial support of the Deutsche Forschungsgemeinschaft under Contract No. Pi 71/18-2 is gratefully acknowledged.

---

[1]J. R. Haynes, Phys. Rev. Lett. 17, 860 (1966).
[2]L. V. Keldysh, in *Proceedings of the Ninth International Conference on the Physics of Semiconductors, Leningrad, 1967,* edited by S. Ryvkin (Nauka, Leningrad, 1968), p. 1303.
[3]For a review of the experimental literature see J. C. Hensel, T. G. Phillips, and G. A. Thomas, in *Solid State Physics,* edited by F. Seitz, D. Turnbull, and H. Ehrenreich (Academic, New York, 1977), p. 88, and references therein.
[4]For a review of the theoretical literature see T. M. Rice, in Ref. 3, p. 1, and references therein.
[5]T. K. Lo, B. J. Feldman, and C. D. Jeffries, Phys. Rev. Lett. 31, 224 (1973).
[6]W. F. Brinkman and T. M. Rice, Phys. Rev. B 7, 1508 (1973); M. Combescot and P. Noziéres, J. Phys. C 5, 2369 (1972).
[7]Ya. Pokrovskii, Phys. Status Solidi A 11, 385 (1972).
[8]R. B. Hammond, T. C. McGill, and J. W. Mayer, Phys. Rev. B 8, 3566 (1976).
[9]B. J. Feldman, H. -h. Chou, and G. K. Wong, Solid State Commun. 24, 521 (1977); 26, 209 (1978).
[10]V. D. Kulakovskii, V. B. Timofeev, and V. M. Edels`htein, Zh. Eksp. Teor. Fiz. 74, 372 (1978) [Sov. Phys.—JETP 47, 193 (1978)].
[11]J. Wagner and R. Sauer, Phys. Status Solidi B 94, 69 (1979).
[12]G. A. Thomas, T. M. Rice, and J. C. Hensel, Phys. Rev. Lett. 33, 219 (1974).
[13]G. A. Thomas, J. B. Mock, and M. Capizzi, Phys. Rev. B 18, 4250 (1978).
[14]A. F. Dite, V. D. Kulakovskii, and V. B. Timofeev, Zh. Eksp. Teor. Fiz. 72, 1156 (1977) [Sov. Phys.—JETP 45, 604 (1977)].
[15]J. Shah, M. Combescot, and A. H. Dayem, Phys. Rev. Lett. 38, 1497 (1977).
[16]G. E. Pikus and G. L. Bir, Fiz. Tverd. Tela (Leningrad) 1, 1642 (1959) [Sov. Phys.—Solid State 1, 136 (1959)].
[17]J. C. Hensel and G. Feher, Phys. Rev. 129, 1041 (1963).
[18]L. Liu, Solid State Commun. 25, 805 (1978); L. Liu and L. S. Liu, *ibid.* 27, 801 (1978).
[19]L. V. Keldysh and A. P. Silin, Zh. Eksp. Teor. Fiz. 69, 1053 (1975) [Sov. Phys.—JETP 42, 535 (1976)]; G. Beni and T. M. Rice, Phys. Rev. B 18, 768 (1978).
[20]E. Guggenheim, J. Chem. Phys. 13, 253 (1945).
[21]D. Bimberg, M. S. Skolnick, and L. M. Sander, in *Proceedings of the Fourteenth International Conference on the Physics of Semiconductors, Edinburgh, 1978,* edited by B. L. H. Wilson (The Institute of Physics, Bristol, 1978), p. 175; D. Bimberg, M. S. Skolnick, and L. M. Sander, Phys. Rev. B 19, 2231 (1979).
[22]T. L. Reinecke and S. C. Ying, Phys. Rev. Lett. 43, 1054 (1979); 43, 1627(E) (1979).
[23]M. Combescot, Phys. Rev. Lett. 32, 15 (1974).
[24]P. Vashishta, S. G. Das, and K. S. Singwi, Phys. Rev. Lett. 33, 911 (1974).
[25]T. L. Reinecke and S. C. Ying, Phys. Rev. Lett. 35, 311 (1975); 35, 547(E) (1975).
[26]T. L. Reinecke, M. C. Lega, and S. C. Ying, Phys. Rev. B 20, 1562 (1979); 20, 5404 (1979).
[27]A. Forchel, B. Laurich, G. Moersch, W. Schmid, and T. L. Reinecke, Phys. Rev. Lett. 46, 678 (1981).
[28]E. Gmelin and U. V. Alpen, Proceedings of the Fifth International Cryogenic Engineering Conference (in press); E. Gmelin, Die Kälte und Klimatechnik 12, 531 (1976).
[29]I. Balslev, Phys. Rev. 143, 636 (1966).
[30]M. A. Tamor and J. P. Wolfe, Phys. Rev. Lett. 25, 1703 (1980).
[31]G. Kirczenow and K. S. Singwi, Phys. Rev. B 21, 3597 (1980).
[32]S. Zwerdling, K. J. Button, B. Lax, and L. M. Roth, Phys. Rev. Lett. 4, 173 (1960).
[33]H. Hasegawa, Phys. Rev. 129, 1029 (1963).
[34]J. Wagner, A. Forchel, and R. Sauer, Solid State Commun. 38, 991 (1981).
[35]J. Wagner, A. Forchel, and R. Sauer, Solid State Commun. 36, 917 (1980).
[36]J. Wagner, W. Schmid, and R. Sauer, Solid State Commun. 32, 1215 (1979)
[37]L. D. Laude, F. H. Pollak, and M. Cardona, Phys. Rev. B 3, 2623 (1971).
[38]G. A. Thomas and T. M. Rice, Solid State Commun. 23, 359 (1977).
[39]J. Shah and A. H. Dayem, Phys. Rev. Lett. 37, 861 (1976).
[40]A. Forchel, B. Laurich, W. Schmid, and M. H. Pilkuhn, in Proceedings of the Fifteenth International Conference on the Physics of Semiconductors, Kyoto,

1980, edited by S. Tanaka [J. Phys. Soc. Jpn. Suppl. A 49, 487 (1980)]; G. Mahler, G. Maier, A. Forchel, B. Laurich, H. Sanwald, and W. Schmid, Phys. Rev. Lett. 47, 1855 (1981).

[41]R. J. Elliott, Phys. Rev. 108, 1384 (1957).

[42]R. B. Hammond and R. N. Silver, Solid State Commun. 28, 993 (1978).

[43]J. C. Merle, M. Capizzi, P. Fiorini, and A. Frova, Phys. Rev. B 17, 4821 (1978).

[44]K. Cho, Opt. Commun. 8, 412 (1973).

[45]M. L. W. Thewalt and J. A. Rostworowski, Solid State Commun. 25, 991 (1978).

[46]W. Schmid, A. Forchel, G. Moersch, and M. H. Pilkuhn, in Proceedings of the Fifteenth International Conference on the Physics of Semiconductors, Kyoto, 1980, edited by S. Tanaka [J. Phys. Soc. Jpn. Suppl. A 49, 465 (1980)].

[47]G. Moersch, Diploma thesis, Stuttgart, 1980 (unpublished).

[48]P. L. Gourley and J. P. Wolfe, Phys. Rev. B 20, 3319 (1979).

[49]M. L. W. Thewalt, J. A. Rostworowski, and G. Kirczenow, Can. J. Phys. 57, 1898 (1979).

[50]P. T. Landsberg, Phys. Status Solidi 15, 623 (1966).

[51]R. W. Martin and H. L. Störmer, Solid State Commun. 22, 523 (1977).

[52]W. Schmid, Phys. Status Solidi B 94, 413 (1979).

[53]P. T. Landsberg, private communication. Owing to its phenomenological basis the Landsberg model cannot be expected to account in detail for the effects of the single- and many-particle excitations which are the physical reason for the line-shape broadening near the reduced band gap. These processes have been considered recently by C. H. Aldrich and R. N. Silver, Phys. Rev. B 21, 600 (1980) and by H. Haug and D. B. Tran Thoai, Phys. Status Solidi B 98, 581 (1980). For the purposes of the present paper, however, the Landsberg model provides an approximate broadening using a comparatively simple mathematical formalism. Hence it seems particularly well suited for the evaluation of EHL line shapes.

[54]M. Combescot, Phys. Status Solidi B 86, 349 (1978).

[55]L. M. Sander and D. K. Fairobent, Solid State Commun. 20, 631 (1976).

[56]R. N. Silver, Phys. Rev. B 11, 1569 (1975); R.M. Westervelt, Phys. Status Solidi B 76, 31 (1976).

[57]G. A. Thomas, A. Frova, J. C. Hensel, R. E. Miller, and P. A. Lee, Phys. Rev. B 13, 1692 (1976).

[58]P. Vashishta. S. G. Das, and K. S. Singwi, Phys. Rev. B 10, 5108 (1974); P. Vashishta, S. G. Das, and K. S. Singwi, Phys. Rev. Lett. 33, 911 (1974). For the exchange-correlation energies the results denoted by "fully self-consistent anisotropic" are used here.

[59]H. L. Störmer, R. W. Martin, and J. C. Hensel, in *Proceedings of the Twelfth International Conference on the Physics of Semiconductors, Rome 1976,* edited by F. G. Fumi (Tipographia Marves, Rome 1976).

[60]G. Kirczenow and K. S. Singwi, Phys. Rev. Lett. 41, 326 (1978).

[61]For Si[6;1] and Si[4;1] n_c, in the uniform plasma approach, lies near a density where there is an artificial discontinuity in the derivatives of $E^{xc}(n)$ resulting from joining the tabulated values of $E^{xc}(n)$ from Ref. 58 at high density to a Wigner fit for lower densities. In order to obtain well-defined inflection points in these two cases the densities at which they are joined are varied somewhat to higher values. This procedure results in an uncertainty in $T_c \sim 2$ K, with the present values expected to be in the lower part of this range (see Ref. 26 for details).

[62]T. L. Reinecke, Phys. Rev. B 18, 2947 (1978).

[63]The values quoted for σ_0 by Reinecke *et al.* in Ref. 26 were inadvertently slightly different from the final values obtained by them which should have read for Si[6;2], Si[2;2], and Si[2;1] 35.0×10^{-4}, 13.1×10^{-4}, and 3.73×10^{-4} erg/cm^2, respectively.

[64]For the correction of the quadratic temperature dependence the following coefficients have been used: 0.49 (Si[6;2]), 0.98 (Si[6;1]), 0.84 (Si[4;1]), and 0.86 (Si[2;1]) in units of meV^{-1}.

[65]K. L. Shaklee and R. E. Nahory, Phys. Rev. Lett. 24, 942 (1970).

[66]In Ref. 27 E_{ex} in Si[6;2] has been approximated by the exciton Rydberg. This leads to the lower value of E_0 reported there.

[67]The data in Refs. 10 and 11 have been obtained at stresses which were lower by about 30% than used in the present work.

[68]V. D. Kulakovskii, I. V. Kukushkin, and V. B. Timofeev, in Proceedings of the Fifteenth International Conference on the Physics of Semiconductors, Kyoto 1980, edited by S. Tanaka [J. Phys. Soc. Jpn. Suppl. A 49, 527 (1980)]; Zh. Eksp. Teor. Fiz. 78, 381 (1980) [Sov. Phys.—JETP 51, 191 (1980)].